

P3.6

A New Direction in Clear-Air Turbulence Forecasting Based on Spontaneous Imbalance Part II: Case Studies and Statistical Results

Donald W. McCann*
McCann Aviation Weather Research, Inc., Overland Park KS

John A. Knox
Faculty of Engineering, University of Georgia, Athens GA

Paul D. Williams
Department of Meteorology, University of Reading, Reading UK

1. INTRODUCTION

To date, clear air turbulence (CAT) forecast techniques have been an amalgamation of mostly empirical rules and equations, most of which are based on perceived connections between observed atmospheric patterns and aircraft turbulence reports. McCann (2001) demonstrates that most techniques look at the environmental setup for CAT as measured directly or indirectly by the Richardson number

$$Ri \equiv \frac{g \frac{d\Theta}{dz}}{\left(\frac{d\mathbf{V}}{dz}\right)^2}$$

where g is the acceleration of gravity, Θ is the potential temperature and \mathbf{V} is the wind velocity. The numerator is the layer's stability (N) squared, and the denominator is the layer's wind shear squared.

Layers above the atmospheric boundary layer are rarely favorable for turbulence because it is necessary for $Ri < 0.25$ for turbulence to form. Assumed in these techniques is some undefined process that locally alters the environment so the atmosphere can become turbulent. The lower the environmental Ri , the higher probability of turbulence. Unfortunately, these techniques overforecast CAT because often low Ri environments are smooth. Moreover, there are many missed significant turbulence reports in higher Ri . The situation is analogous to thunderstorm forecasting only considering conditional instability. Indeed, the thunderstorm probability increases with a lower Lifted Index,

but successful thunderstorm forecasts include consideration of convection-initiating triggers. Similarly, CAT forecasting techniques that include a trigger analysis should reduce the uncertainty of environment-only techniques.

Gravity waves, which are ubiquitous in the atmosphere, alter both the environmental wind shear and the stability as they move through. McCann (2001) shows that, under the influence of a gravity wave, the local Richardson number (Ri_L) becomes

$$Ri_L = Ri_E \frac{1 + \hat{a} \cos \varphi}{\left(1 + Ri_E^{1/2} \hat{a} \sin \varphi\right)^2}$$

where Ri_E is the environmental Richardson number, φ is the gravity wave phase angle, and \hat{a} is a non-dimensional wave amplitude,

$$\hat{a} = \frac{aN}{|\mathbf{V} - \mathbf{c}|}$$

created by multiplying the actual wave amplitude (a) by the stability and dividing by the Doppler-adjusted wind speed, $|\mathbf{V} - \mathbf{c}|$, where \mathbf{c} is the wave phase velocity. There are sufficient observations/numerical model forecasts of the wind and temperature to compute environmental stability, wind shear, and Ri_E . The gravity wave amplitude and phase velocity are unknowns that make computing Ri_L difficult.

Spontaneous imbalance in the atmosphere generates gravity waves (Ford 1994; Medvedev and Gavrilov 1995). It is not difficult to diagnose and forecast regions and altitudes of spontaneous imbalance from gridded numerical data (Part I, Knox et al. 2008). Therefore, we are beginning to get a handle on locations of gravity wave triggers, the illusive ingredient that will

* Corresponding author address: Donald McCann, McCann Aviation Weather Research, Inc. 7306 157th Terrace, Overland Park, KS 66223; e-mail: don@mccannawr.com

allow forecasters to completely analyze the atmosphere for favorable CAT conditions.

Part I (Knox et al. 2008) outlines how to apply spontaneous imbalance theory to CAT forecasting. In this Part II two case studies show that the theory may be applied to all flight altitudes above the boundary layer. Additionally, more than 9000 turbulence pilot reports were collected during the 2005-2006 winter and were compared with our spontaneous imbalance theory application. The statistical results are very exciting and point to improved CAT forecasts in the near future.

2. Two Case Studies

a. Mid and Upper Level Turbulence

On 9 March 2006, a significant CAT outbreak occurred over areas of the central Mississippi River Valley. In the two hours between 0000 UTC and 0200 UTC 10 March nearly three dozen pilot reports (PIREPs) of CAT were received, including eight reports of severe or moderate-to-severe turbulence. Moderate or greater turbulence occurred in some portions of the area in a very deep layer at all flight levels between FL110 and FL410.

Using the 1-hour RUC2 forecast from 0000 UTC 10 March 2006, we calculate the turbulent kinetic energy (TKE) dissipation (ϵ) as outlined in Part I (Knox et al. 2008). Figure 1 shows the computed TKE dissipation for the flight levels above FL110 to FL390 in 2000 ft intervals and the reported PIREPs. The agreement between regions of maximum TKE dissipation and the PIREPs is considerable. Nearly every MODERATE or greater turbulence PIREP was horizontally within 50 km of a grid point of $\epsilon > .10 \text{ j s}^{-1}$.

Figure 2 shows the Lighthill-Ford gravity wave radiation and the Richardson number for two levels, near 200 mb or FL390 and near 550 mb or FL150. At each level note the broad areas of $Ri < 1$, the usual, overforecast size of this environment-only indicator in a CAT outbreak. Also usual are some significant CAT reports outside the low Ri areas. Not only does considering the Lighthill-Ford radiation trigger mechanism reduce the threat areas forecasted with Ri alone, but also it correctly extends the threat into areas where the environment is less favorable. This illustrates the characteristics of McCann's (2001) ingredients-based CAT forecast method.

b. Low level turbulence

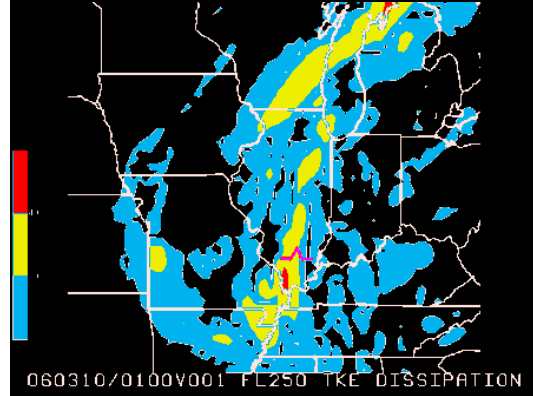
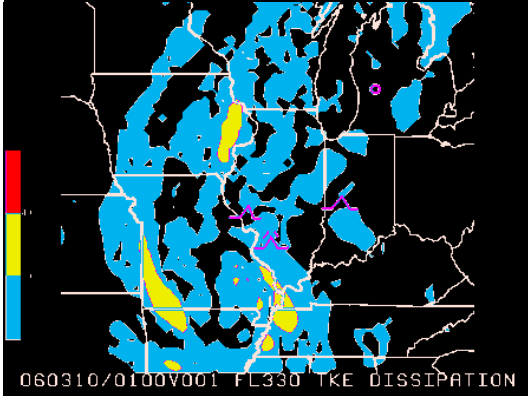
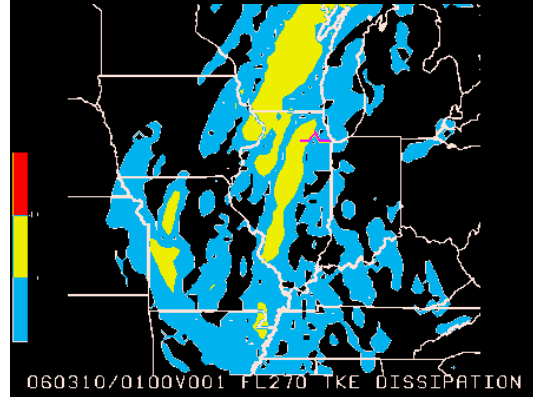
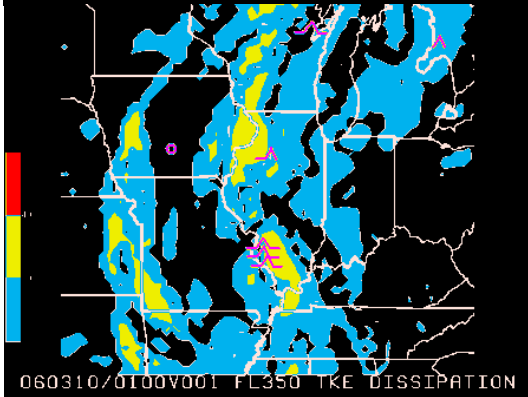
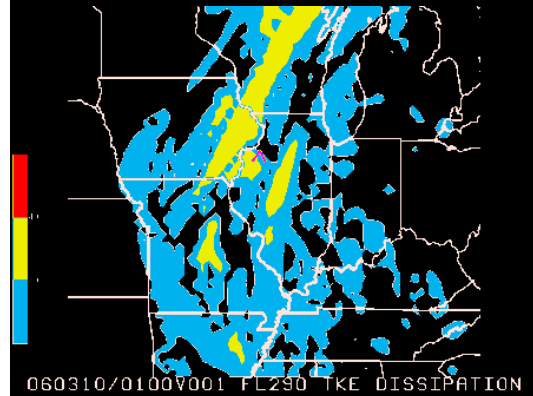
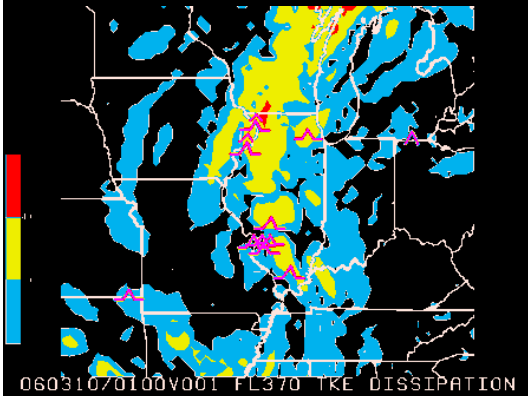
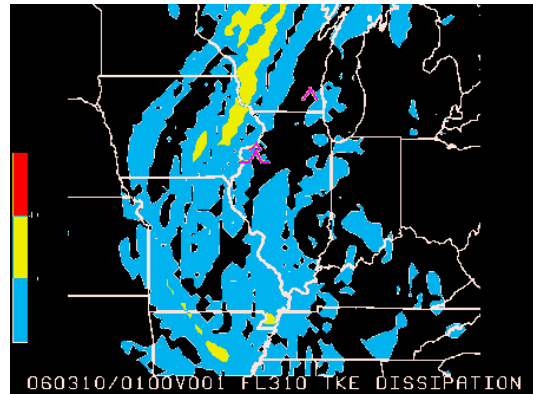
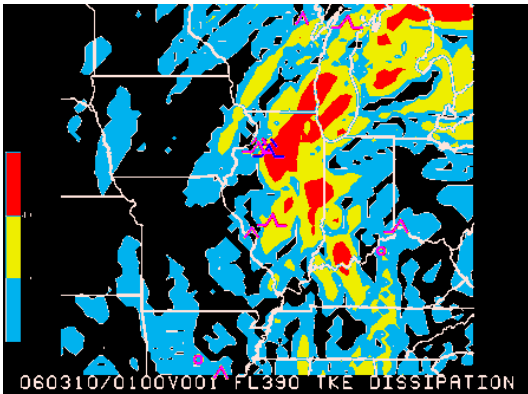
In the morning of 28 December 2005, significant turbulence occurred below FL80 in the Pacific Northwest. Although there were only three PIREPs in the area between 1500 UTC and 1700 UTC, there apparently were earlier reports because the Aviation Weather Center had issued a severe turbulence SIGMET. And because of the SIGMET, there were probably fewer than usual aircraft flying.

Figure 3 shows three levels below FL80 of the calculated TKE dissipation and the reported PIREPs. Again, the higher TKE dissipation values capture the significant turbulence pilot reports.

Figure 4 shows the Lighthill-Ford gravity wave radiation and the low Richardson numbers. Note the large area of $Ri < 1$. The Lighthill-Ford radiation is a maximum along a cold front (not shown) that is moving through the area. Again, the additional ingredient, a gravity wave trigger, reduced the threat area for this time compared with just considering the environmental conditions.

3. Verification Results

McCann's (2001) ingredient-based method with a Lighthill-Ford gravity wave trigger outlined in Part 1 (Knox et al. 2008) is now used to diagnose the occurrence of CAT during a 144-day period using the 20-km output from the 13 km RUC2 numerical model. Layer TKE dissipation rates calculated from the 1-hour forecasts from the 1500 UTC model run (valid at 1600 UTC) for each day from 3 November 2005 to 26 March 2006 are validated with 9542 text PIREPs from 1500 UTC to 1700 UTC above the planetary boundary layer. PIREPs in convection (as determined subjectively from satellite imagery) or in mountain waves (as determined by the MWAVE algorithm; McCann 2006) were not included in the database. The planetary boundary layer height was calculated from BLTURB, a boundary layer turbulence algorithm based on McCann (1999). Because the 0-hour analyses showed some extraneous noise in our calculations, we feel the 1-hour forecasts are a more accurate representation of the atmosphere without errors introduced by the model itself. The maximum TKE dissipation rate in the layer with the FL within 50 km of the pilot report was matched with the subjective PIREP turbulence intensity.



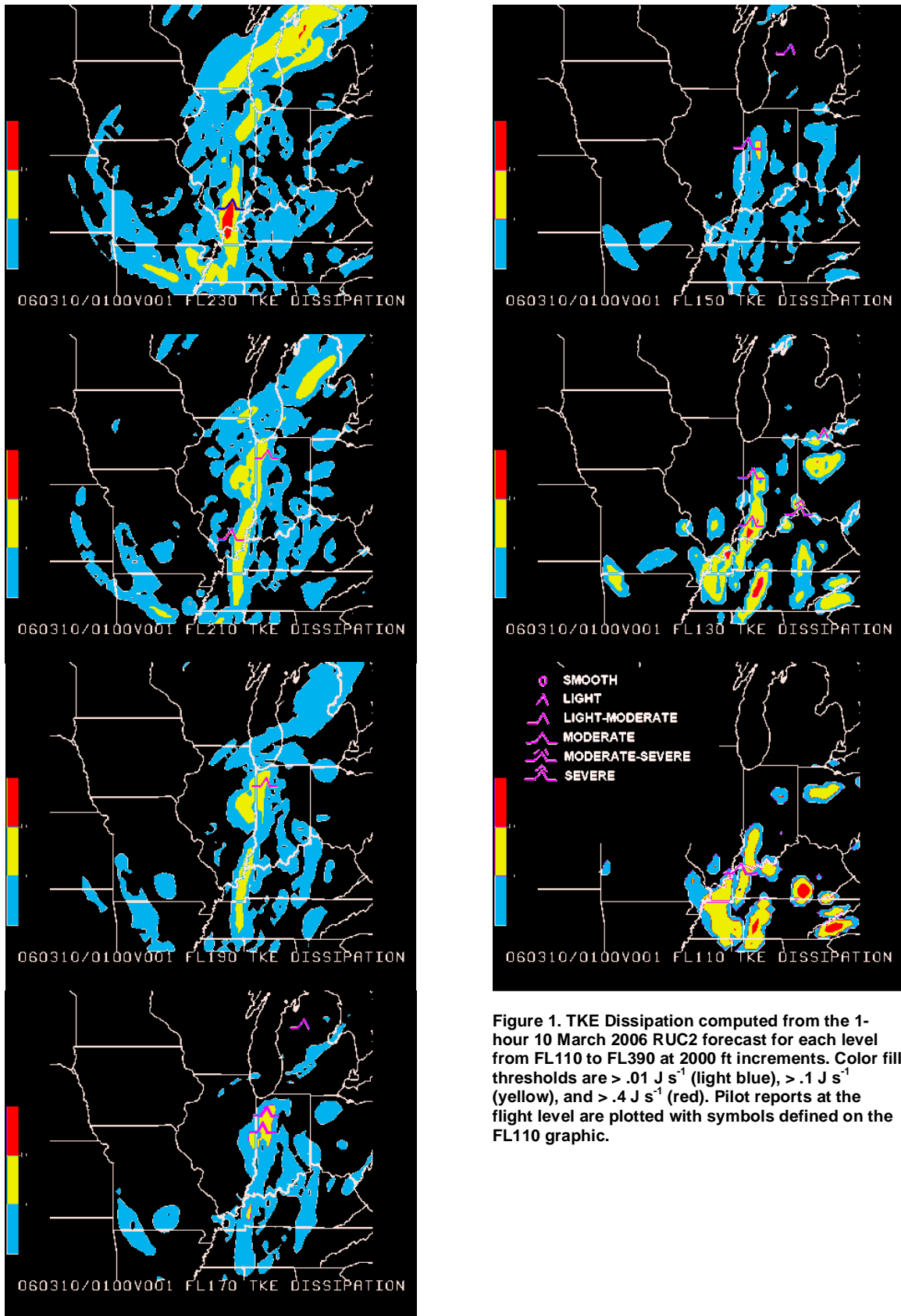


Figure 1. TKE Dissipation computed from the 1-hour 10 March 2006 RUC2 forecast for each level from FL110 to FL390 at 2000 ft increments. Color fill thresholds are $> .01 \text{ J s}^{-1}$ (light blue), $> .1 \text{ J s}^{-1}$ (yellow), and $> .4 \text{ J s}^{-1}$ (red). Pilot reports at the flight level are plotted with symbols defined on the FL110 graphic.

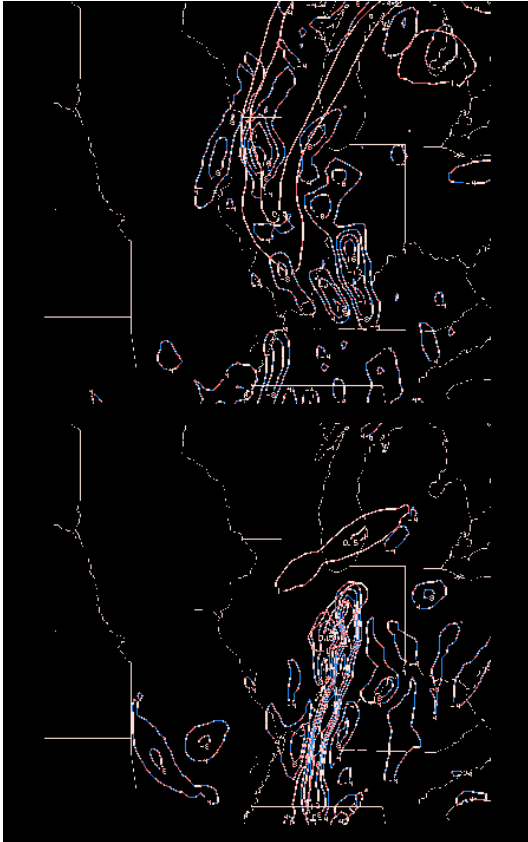


Figure 2. Lighthill-Ford gravity wave radiation (light blue) and Richardson number less than 1 (pink) for top) the 200:225 mb layer or FL370 and bottom) the 550:575 mb layer or FL150 from the 1-hour 0000 UTC 10 March 2006 RUC2 forecast.

We created a set of 2 X 2 contingency tables by varying the threshold chosen to make a yes-or-no forecast decision and then compared them with observed yes-or-no conditions (Mason 1982). The Heidke Skill Score (HSS; Doswell et al. 1990) is one of many summary measures for 2 X 2 contingency tables. Its strength over other summary measures is its ability to account for rare events. Because PIREPs are sparse and not random (they tend to report positive turbulence), the false alarm and miss categories may be uncertain. Therefore, the absolute value of the HSS is not likely accurate, but it may be compared within a HSS set to assess which threshold has the highest skill.

Figure 5 shows the HSS for our application of Lighthill-Ford theory to CAT forecasting during our verification period. It reveals a positive forecast skill for all turbulence intensities. Especially noteworthy is that the

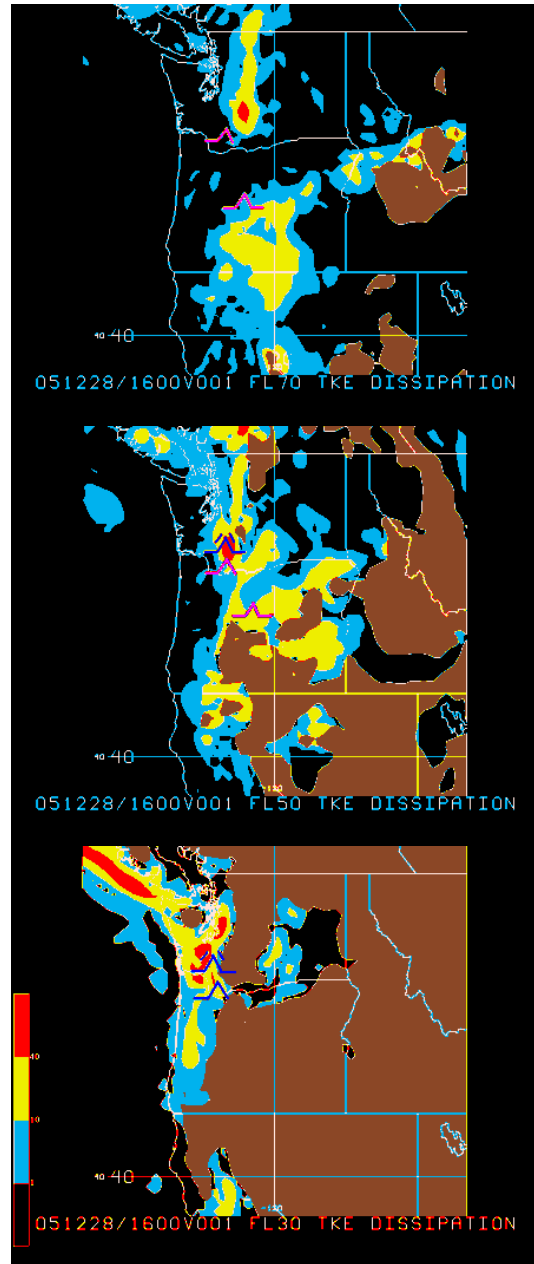


Figure 3. Same as Fig. 1 except for FL70, FL50, and FL30 for the 1-hour 28 December 2005 1500 UTC RUC2 forecast. Color fill thresholds and pilot report symbols are the same as Fig. 1. Brown color fill areas are below the ground.

highest score for the differentiation between no turbulence and positive turbulence is for a zero threshold. In other words, when there is positive TKE dissipation forecast, aircraft will likely feel some turbulence. At moderate and severe intensities the HSS peaks with higher TKE dissipation; this indicates that the higher the forecast rate, the stronger the expected turbulence. With these results, we chose the color fill thresholds of $.01 \text{ j s}^{-1}$, $.1 \text{ j s}^{-1}$, and $.4 \text{ j s}^{-1}$

as “useful” values to represent LIGHT, MODERATE, and SEVERE turbulence, respectively, in Figures 1 and 3.

Figure 6 shows the turbulence intensity forecast skill for various altitude layers. LIGHT and MODERATE turbulence are better forecast in lower levels while SEVERE turbulence is better forecast in upper levels. We think this result is partly because smaller aircraft fly at lower levels and more likely to report a higher intensity than a larger aircraft in the same conditions. Thus, more severe turbulence at lower levels is reported in lower TKE dissipation values than at upper levels. On the other hand, many larger aircraft appear to have reported moderate turbulence in regions with lesser TKE dissipation.

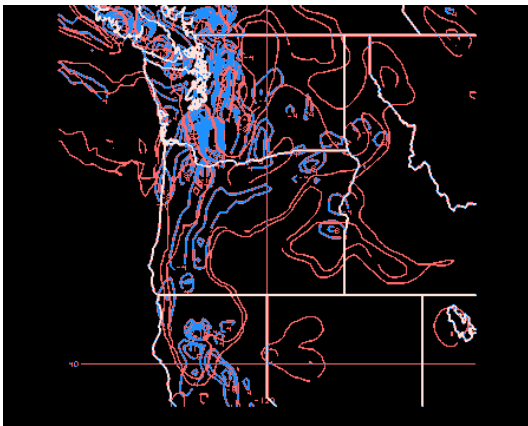


Figure 4. Same as Fig. 2 except for the 850:875 mb layer or FL50 from the 1-hour 1500 UTC 28 December 2005 RUC2 forecast.

We can compare our method with the Graphical Turbulence Guidance (GTG; Sharman et al. 2006) with data from the same time period at <http://rtvs.noaa.gov>. Their data is for PIREPs \geq FL200 and only allows for a MODERATE intensity comparison. The two datasets differ slightly in that ours is a 1-hour forecast and theirs is a 0-hour forecast. Also theirs only considers SMOOTH PIREPs as “no” observations while ours considers LIGHT and LIGHT-MODERATE as “no” observations. Figure 7 shows the Relative Operating Characteristic (ROC) curves for both methods. The Lighthill-Ford method’s ROC is much closer to the upper right corner than GTG’s indicating our new method is more skillful.

Moreover GTG’s skill for MODERATE maximizes at their 0.25 (HSS = .322), which is their stated value for LIGHT. Other data (not shown) suggest that GTG’s maximum skill for all

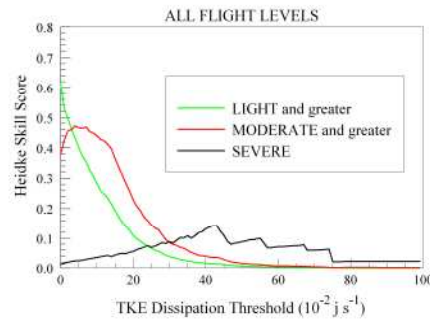


Figure 5. Heidke Skill Scores at a range of TKE dissipation thresholds for all flight levels at three turbulence intensities.

intensities is also their 0.25 value. Therefore, GTG has no real discriminating skill. At their stated value for MODERATE (0.5) their HSS is only .132. Data also show zero skill at their stated value for SEVERE (0.75).

4. Conclusions

We have implemented McCann’s (2001) ingredients-based turbulence method using Lighthill-Ford theory as an indicator of gravity wave triggers. It has the ability to forecast turbulence intensity at all flight levels above the planetary boundary layer. Figures 1 and 3 show sample displays.

Our method really shines when considering the season-long statistics. There is positive skill for all turbulence intensities. Aircraft turbulence intensity appears to be positively correlated with forecast TKE dissipation.

The U.S. Federal government goal for CAT forecast techniques is for a probability of detection for MODERATE or greater turbulence greater than 0.8 with a probability of detection of SMOOTH reports greater than 0.85 (Sharman et al. 2006). Our application reaches this goal with a PODyes for MODERATE or greater turbulence of .831 and a PODyes of SMOOTH of .851 at a zero threshold. However, this is our threshold for LIGHT. At our recommended threshold for MODERATE ($.1 \text{ j s}^{-1}$), the PODyes is only .487.

Our method shows a substantial skill increase over current popular methods including the most skillful algorithm, the Graphical Turbulence Guidance.

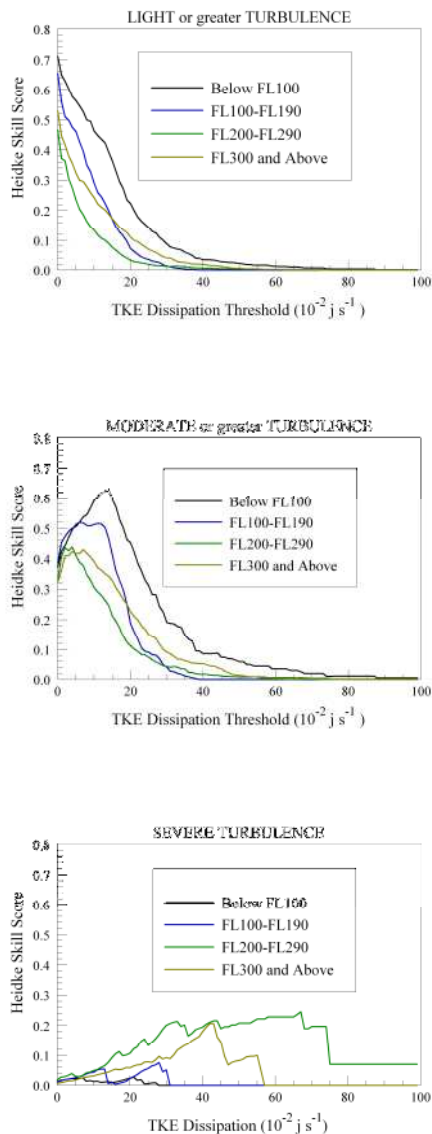


Figure 6. Heidke Skill Scores for LIGHT or greater, MODERATE or greater, and SEVERE turbulence versus TKE Dissipation thresholds in four altitude ranges.

We are calling our method a new direction in CAT forecasting because heretofore most methods have only considered favorable environmental conditions as represented by the Richardson number. They have assumed that something comes along to initiate the turbulence. We have identified Lighthill-Ford gravity wave radiation as an initiator. Although GTG considers some gravity wave triggers, it cannot be considered a new direction because it combines them in an unphysical manner with the environmental conditions.

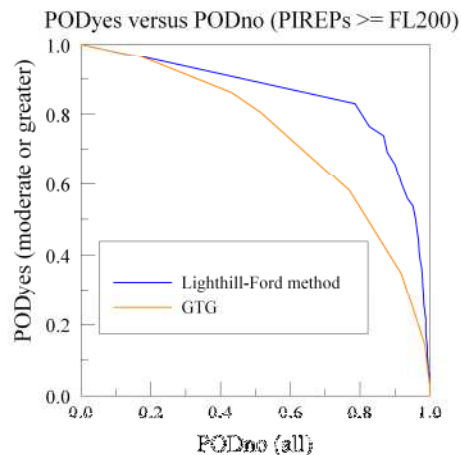


Figure 7. Relative Operating Characteristic curves for MODERATE or greater CAT PIREPs FL200 or higher for the Graphical Turbulence Guidance product and for our Lighthill-Ford method.

Aviation professionals and the flying public need better forecasts to help reduce the substantial cost due to the turbulence. We conclude by calling for an immediate implementation of our method and research to improve upon it.

REFERENCES

- Doswell III, C. A., R. Davies-Jones, and D. Keller, 1990: On summary measures of skill in rare event forecasting based on contingency tables. *Wea. Forecasting*, **5**, 576-585.
- Ford, R., 1994: Gravity wave radiation from vortex trains in rotating shallow water. *J. Fluid Mech.*, **281**, 81-118.
- Knox, J.A., D.W. McCann, and P.D. Williams, 2008: A new direction in clear-air turbulence forecasting based on spontaneous imbalance Part I: Application of theory, Proc. 13th Aviation, Range, and Aerospace Meteorology, New Orleans, LA, paper P3.4
- Mason, L., 1982: A model for assessment of weather forecasts. *Australian Meteorological Magazine*, **30**, 291-303.
- McCann, D. W., 1999: A simple turbulent kinetic energy equation and aircraft boundary

- layer turbulence. *Nat. Wea. Digest*, **23(1,2)**, 13-19.
- McCann, D. W., 2001: Gravity waves, unbalanced flow, and clear air turbulence. *Nat. Wea. Digest*, **25(1,2)**, 3-14.
- McCann, D. W., 2006: Diagnosing and forecasting aircraft turbulence with steepening mountain waves. *Nat. Wea. Digest*, **30**, 77-92.
- Medvedev, A.S., and N.M. Gavrilov, 1995: The nonlinear mechanism of gravity wave generation by meteorological motions in the atmosphere. *J. Atmos. Terr. Phys.*, **57**, 1221-1231.
- Sharman, R., C. Tebaldi, G. Wiener, and J. Wolff, 2006: An integrated approach to mid- and upper-level turbulence forecasting. *Wea. Forecasting*, **21**, 268-287.